Developmental Cell, Vol. 9, 237–248, August, 2005, Copyright ©2005 by Elsevier Inc. DOI 10.1016/j.devcel.2005.07.002

An Essential Function of the *C. elegans* Ortholog of TPX2 Is to Localize Activated Aurora A Kinase to Mitotic Spindles

Nurhan Özlü,[1,*] Martin Srayko,[1] Kazuhisa Kinoshita,[1] Bianca Habermann,[2] Eileen T. O'Toole,[4] Thomas Müller-Reichert,[1] Natalie Schmalz,[1] Arshad Desai,[1,3] and Anthony A. Hyman[1,*]

[1]Max Planck Institute of Molecular Cell Biology and Genetics
Pfotenhauerstrasse 108
Dresden 01307
Germany

[2]Scionics Computer Innovation
Pfotenhauerstrasse 110
Dresden 01307
Germany

[3]Ludwig Institute for Cancer Research
Department of Cellular and Molecular Medicine
University of California, San Diego
9500 Gillman Drive
La Jolla, California 92093

[4]Boulder Laboratory for 3D Electron Microscopy of Cells
University of Colorado
Boulder, Colorado 80309

Summary

In vertebrates, the microtubule binding protein TPX2 is required for meiotic and mitotic spindle assembly. TPX2 is also known to bind to and activate Aurora A kinase and target it to the spindle. However, the relationship between the TPX2-Aurora A interaction and the role of TPX2 in spindle assembly is unclear. Here, we identify TPXL-1, a *C. elegans* protein that is the first characterized invertebrate ortholog of TPX2. We demonstrate that an essential role of TPXL-1 during mitosis is to activate and target Aurora A to microtubules. Our data suggest that this targeting stabilizes microtubules connecting kinetochores to the spindle poles. Thus, activation and targeting of Aurora A appears to be an ancient and conserved function of TPX2 that plays a central role in mitotic spindle assembly.

Introduction

Chromosome segregation takes place on a bipolar, microtubule-based mitotic spindle. During interphase, microtubules radiate from the centrosome, a microtubule-nucleating center. As cells enter mitosis, microtubules reorganize to build a mitotic spindle (reviewed in Wittmann et al., 2001). Microtubules in a mitotic spindle come from two different sources. One source is microtubules nucleated by the centrosome; these grow out from the centrosomes and associate with chromosomes, where they are stabilized. Another source is microtubules nucleated around chromosomes. These microtubules self-organize into two spindle poles through the action of microtubule-based motors. The relative contributions of these two different pathways vary in different systems (reviewed in Gadde and Heald, 2004).

Mitotic spindles assemble with a characteristic length and shape, which differs in various cell types and organisms. Spindle length can be influenced by the dynamic balance between microtubule stabilization and destabilization within the spindle (Karsenti and Vernos, 2001; Mitchison et al., 2005; Tournebize et al., 2000); changing the global parameters of microtubule dynamics alters the length of spindles (Scholey et al., 2003). In addition, motor proteins acting on microtubules can regulate the length and shape of spindles (Sharp et al., 2000). To date, we understand little about the integration of these different mechanisms in the regulation of spindle length and size.

TPX2, a microtubule-associated protein, is required for mitotic spindle assembly in human cells and *Xenopus* egg extracts (reviewed in Gruss and Vernos, 2004). In *Xenopus* meiotic egg extracts, TPX2 stimulates the formation of microtubules around chromosomes (Groen et al., 2004; Gruss et al., 2001; Schatz et al., 2003). However, we do not know what the role of TPX2 is in mitosis.

A clue as to the possible function of TPX2 came with the discovery that TPX2 binds to the mitotic kinase Aurora A and stimulates its activity (Eyers et al., 2003; Trieselmann et al., 2003; Tsai et al., 2003). In human cells, TPX2 is required for localization of Aurora A to spindles (Kufer et al., 2002). However, the cell cycle arrest phenotype of Aurora A has made it difficult to determine whether an essential function of TPX2 is to localize Aurora A or whether it has other roles (Hirota et al., 2003; Prigent and Giet, 2003). Further complicating the relationship between TPX2's function in spindle assembly and its binding to Aurora A is recent work in *Xenopus* extracts suggesting that the non-Aurora A targeting domain is able to rescue extracts depleted of TPX2 (Brunet et al., 2004).

Although the analysis of TPX2 in mitotic cells indicates a role in spindle function or integrity, it is unclear how these spindle defects manifest over the course of the assembly process. In principle, studying TPX2 in a genetically tractable organism such as yeast, *C. elegans*, or *Drosophila* could help to answer some of these questions. However, to date no TPX2 homolog has been identified in invertebrates. *C. elegans* is an ideal system to identify and study the potential function of Aurora A activators, because Aurora A has a very severe defect in spindle assembly and apparently gives no cell cycle arrest. Here, we use *C. elegans* early embryos to identify TPXL-1, the first known invertebrate ortholog of TPX2. Our results show that the function of TPXL-1 is to activate and localize Aurora A to the mitotic spindle. Comparison of TPXL-1 and Aurora A function further indicates that TPXL-1-mediated activation and localization of Aurora A is necessary to stabilize microtubules connecting kinetochores to spindle poles. These results provide mechanistic insight into

*Correspondence: ozlu@mpi-cbg.de (N.O.); hyman@mpi-cbg.de (A.A.H.)

how the conserved TPX2 protein family contributes to spindle assembly.

Results

TPXL-1 Is a TPX2 Ortholog in *C. elegans* Embryos

To find a *C. elegans* ortholog for TPX2, we screened through genes required for spindle assembly. We identified an uncharacterized gene ORF (Y39G10AR.12) required for spindle assembly, which was initially reported in a Chromosome I RNA interference (RNAi) screen (Fraser et al., 2000). After RNAi of this gene, the separated centrosomes collapse together shortly after nuclear envelope break down (NEBD) and fail to form a robust spindle (Figures 1A and 1B). We name this gene *tpxl-1* (*TPX*2-*l*ike, for reasons stated below).

Sequence alignment with TPX2 showed homology within the N terminus (residues 1–60) (Figures 2A and 2B). This short region of homology was significant because the N-terminal 43 residues of TPX2 have been shown to be sufficient for binding and activating Aurora A kinase (Bayliss et al., 2003). We also determined that the N terminus of TPXL-1 similarly binds *C. elegans* Aurora A, AIR-1. AIR-1 specifically bound to and eluted from a wild-type GST::N-terminal-TPXL-1 (aa 1–63) column but did not bind to mutated TPXL-1 constructs, which should block the interaction between TPXL-1 and AIR-1, based on comparisons to TPX2 (Bayliss et al., 2004, 2003; Eyers and Maller, 2004) (Figure 2C; confirmed by mass spectrometry). In agreement with the results shown above, a genome-wide Yeast Two-Hybrid screen of *C. elegans* proteins also identified an interaction between TPXL-1 and AIR-1 (Li et al., 2004).

If TPXL-1 is an ortholog of TPX2, then it should also stimulate the kinase activity of AIR-1. We found that addition of TPXL-1(1–63) dramatically increased the phoshorylation of Histone H3 by AIR-1 kinase, whereas the TPXL-1(1–63) mutant proteins had no effect (Figure 2D). Therefore, we conclude that TPXL-1 binds to and activates Aurora A kinase and that TPXL-1 is an ortholog of vertebrate TPX2.

Interaction of TPXL-1 with AIR-1 Is Required for Spindle Assembly

In human cells, TPX2 is required to localize Aurora A to spindles (Kufer et al., 2002). To test whether *C. elegans* TPX2 is also required to localize *C. elegans* Aurora A, we raised and affinity-purified antibodies to TPXL-1. On Western blots, Anti-TPXL-1 antibodies recognized a single band of approximately 75 kDa that disappeared in *tpxl-1(RNAi)* worm lysate (see Figure S1A in the Supplemental Data available with this article online). Both TPXL-1 immunostaining and live imaging of embryos expressing TPXL-1::GFP showed that TPXL-1 colocalizes with AIR-1 (Figure 3A, see also Movies S3 and S4). We tested for interdependency of their respective intracellular-localization patterns. In *tpxl-1(RNAi)* embryos, AIR-1 was no longer detected on astral microtubules but instead colocalized with γ-tubulin (Figure 3A, see also Movie S5). In contrast, in *air-1(RNAi)* embryos, TPXL-1 was still detected on microtubules (Figure 3B).

Is the main function of TPX2 in spindle assembly to interact with Aurora A? The consequences of depleting

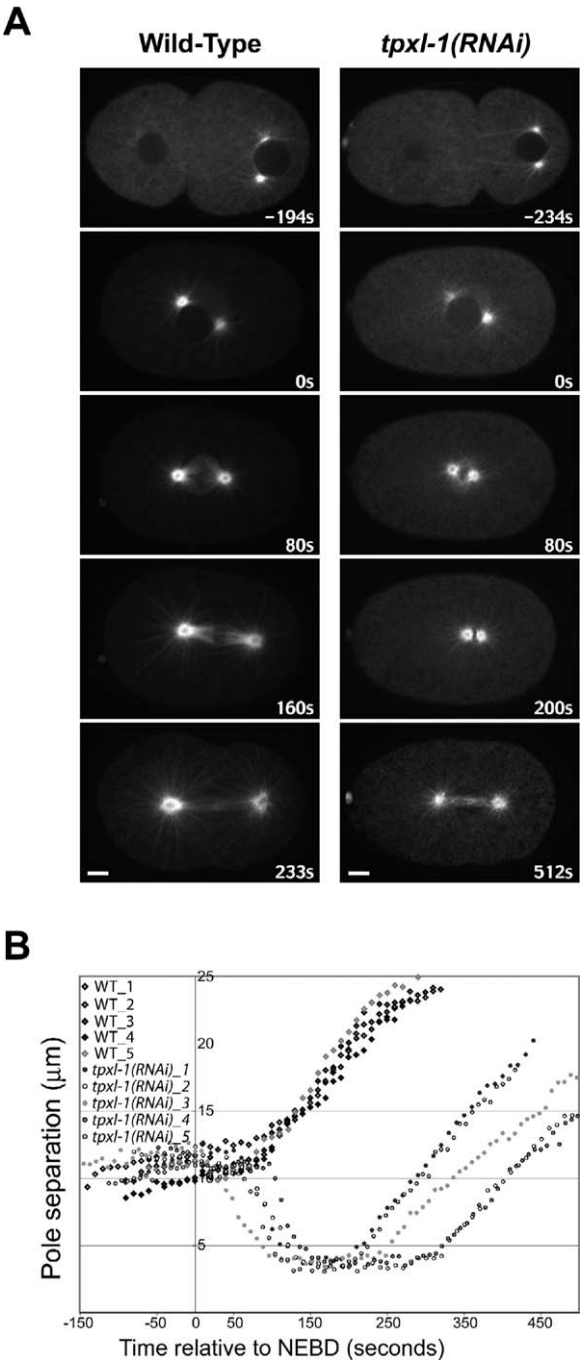

Figure 1. Spindle Poles Collapse in Embryos Depleted of TPXL-1

(A) Summarization of spinning disk confocal time-lapse movies taken from wild-type (left) and *tpxl-1(RNAi)* (right) embryos expressing GFP::β-tubulin. Times are in seconds relative to NEBD. In the TPXL-1-depleted embryos, centrosomes separate as in wild-type (–234 s). Upon NEBD (0 s), separated centrosomes collapse together (80 s and 200 s). After wild-type embryos initiate anaphase, the spindle in *tpxl-1(RNAi)* embryos elongates but reaches a shorter total spindle length (512 s). See also Movies S1 and S2.

(B) Pole-to-pole distances were measured in five wild-type (diamonds) and five *tpxl-1(RNAi)* (circles) embryos. Bars: 5 μm.

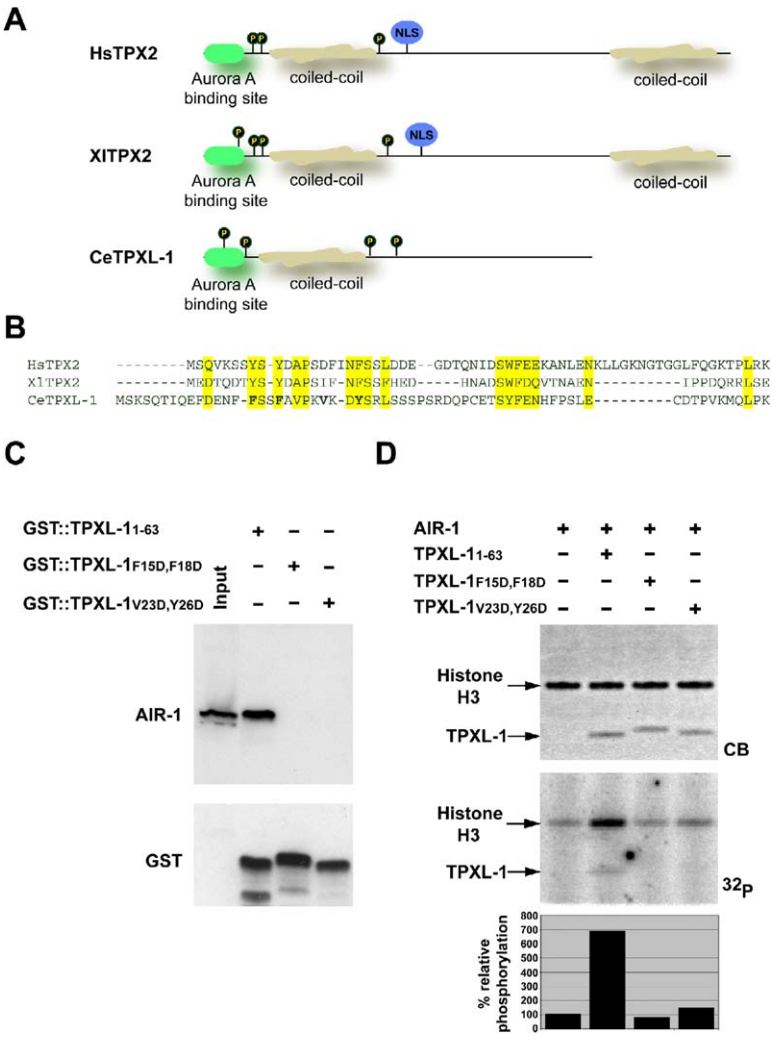

Figure 2. TPXL-1 Binds to and Stimulates AIR-1 Kinase

(A) Common features of *C. elegans* (Ce), *Homo sapiens* (Hs), and *Xenopus laevis* (Xl) TPX2 proteins. TPXL-1 and TPX2 share homology in the minimum Aurora A binding site (green box, aa 1–43; Bayliss et al., 2003). TPX2 contains two coiled-coil domains (Hs aa 213–247 and 664–729; Xl aa 171–216 and 637–696). TPXL-1 possesses one N-terminal coiled-coil domain (aa 150–173). Consensus Aurora A phosphorylation sites (consensus sequence: (RX[S/T]); Cheeseman et al., 2002) in the N termini of TPX2 and TPXL-1 are shown by black circles (aa positions in TPXL-1 are 30, 68, 149, and 154). A functional nuclear-localization signal in vertebrates (Schatz et al., 2003) is indicated by blue circles.

(B) Multiple sequence alignment of Aurora A binding domain and the N-terminal regions of TPXL-1 from *C. elegans* (Ce) with TPX2 from human (Hs) and *Xenopus* (Xl). The conserved residues are boxed in yellow. Residues that are mutated in (C) and (D) are indicated with bold lettering.

(C) GST-pulldown assay shows that AIR-1 binds to GST::TPXL-1 (1–63). GST fusions were expressed in *E. coli*, bound to glutathione resin, incubated in worm extract, and eluted with glutathione. Elutions were fractionated by SDS-PAGE and analyzed via Western blotting with anti-AIR-1 (top) and anti-GST (bottom) antibodies. AIR-1 can be detected as a single band (40 kDa) in worm extracts and in the GST::TPXL-1 (1–63) pulldown, but not in the pulldowns performed with the TPXL-1 (1–63) mutants.

(D) TPXL-1 (1–63) stimulates AIR-1 kinase activity. In vitro phosphorylation of histone H3 (determined by γ[^{32}P]-ATP levels) in the presence of AIR-1 and either TPXL-1 (1–63) or the indicated TPXL-1 (1–63) mutants. Coomassie blue stain and autoradiograph of the SDS-PAGE gel are shown. For quantification of histone H3 phosphorylation (bottom), the value of 100% was assigned to the phosphorylation of Histone H3 in the presence of only AIR-1.

TPXL-1 on spindle assembly may reflect both AIR-1-dependent and AIR-1-independent functions. To specifically analyze AIR-1-dependent functions, we generated transgenes expressing either wild-type TPXL-1 or the N-terminal mutant that does not interact with AIR-1 (see Figures 2C and 2D). To specifically remove endogenous TPXL-1 function, the introduced transgenes were engineered to be resistant to RNAi by insertion of silent mutations in the N terminus (Figure 4A). Indeed, immunoblotting of wild-type and mutant transgenic worms showed that *tpxl-1(RNAi)* specifically depleted the endogenous TPXL-1 without affecting RNAi-resistant forms (Figure S1B). In the presence of the wild-type transgene, RNAi of the endogenous *tpxl-1* gene did not affect expression of the transgene and the spindle collapsed only slightly (Figures 4B and 4C). In the presence of the mutated transgene, RNAi of the endogenous *tpxl-1* gene did not affect expression of the transgene (Figure 4B) but the spindle completely collapsed with a similar profile as TPXL-1-depleted embryos (Figures 4B and 4C). Furthermore, depletion of TPXL-1 prevents AIR-1 localization on spindle and astral microtubules and leads to AIR-1 collapse into the same domain of the centrosome as γ-tubulin (Figure 3A). Similarly, in the presence of the mutated transgene, after RNAi of the endogenous *tpxl-1* gene, AIR was no longer detected on microtubules or the peripheral centrosomal region but was collapsed to the inner centrosomal region (Figure 4D). Thus, the interaction between TPXL-1 and AIR-1 targets AIR-1 to the microtubules. The specificity of this experiment suggests that an essential function of TPXL-1 is to target AIR-1 to the spindle microtubules.

To confirm this idea, we compared the phenotypes of TPXL-1 and AIR-1 depletion by RNA interference. AIR-1 is required for cell polarity, centrosome maturation, maintenance of separated centrosomes after NEBD, formation of a robust microtubule aster, spindle

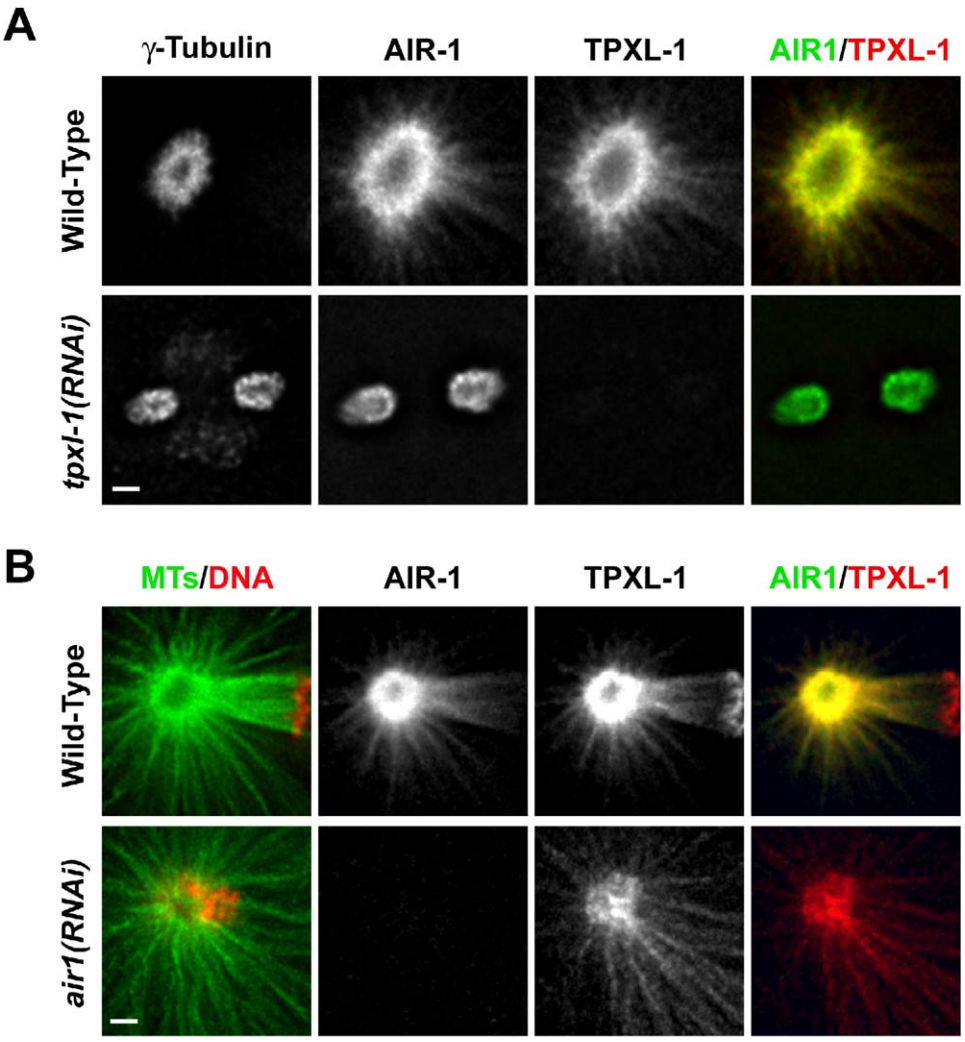

Figure 3. TPXL-1 Is Required for Targeting *C. elegans* Aurora A (AIR-1) to the Spindle

(A) TPXL-1 and AIR-1 colocalize at the centrosome, and TPXL-1 is required for AIR-1 to extend outward from the core centrosome along microtubules. The top row shows a high-magnification view of one centrosome from a wild-type metaphase embryo stained for γ-tubulin, AIR-1, and TPXL-1. AIR-1 and TPXL-1 colocalize on the outer centrosomal layer and extend along centrosomal microtubules. The bottom row shows both mitotic centrosomes in a *tpxl-1(RNAi)* embryo. AIR-1 collapses to colocalize with γ-tubulin after depletion of TPXL-1 and does not extend along centrosomal microtubules.

(B) TPXL-1 still extends onto microtubules in AIR-1-depleted embryos. High-magnification view of one centrosome from a wild-type embryo at the onset of anaphase (top) and an *air-1(RNAi)* embryo (bottom) stained for microtubules (green) and DNA (red) (left), AIR-1 (green), and TPXL-1 (red) (right). All images are single z sections of deconvolved wide-field data sets. Bars: 1 μm.

assembly, and anaphase spindle elongation (Hannak et al., 2001, 2002; Schumacher et al., 1998). Table 1 summarizes the phenotypic comparison of AIR-1- and TPXL-1-depleted embryos. Formation of the PAR domains (data not shown), anaphase spindle elongation (Figures 1A and 1B), and centrosome maturation (Figures S2A and S2B) were normal after depletion of TPXL-1. In both wild-type and *tpxl-1(RNAi)* embryos, γ-tubulin accumulated with similar rates (Figure S2A and S2B). Although this result suggested that centrosome maturation was normal, formation of a robust aster was defective after depletion of TPXL-1 (Figure S2C). The phenotypic differences between *tpxl-1(RNAi)* and *air-1(RNAi)* could represent weakened AIR-1 activity rather than complete loss of a subset of AIR-1 functions. However, we never observe the characteristic *tpxl-1(RNAi)* phenotype with even partial loss of AIR-1 function (data not shown). Therefore, it seems likely that TPXL-1 is required for a subset of AIR-1 activities, namely formation of a robust mitotic aster and assembly of a mitotic spindle.

The Role of TPXL-1 in Spindle Assembly Is Independent of Chromatin-Stimulated Microtubule Assembly

Why do spindles collapse after depletion of TPXL-1? In *Xenopus* egg extracts, TPX2 stimulates chromatin-dependent microtubule nucleation in a Ran-GTP-depen-

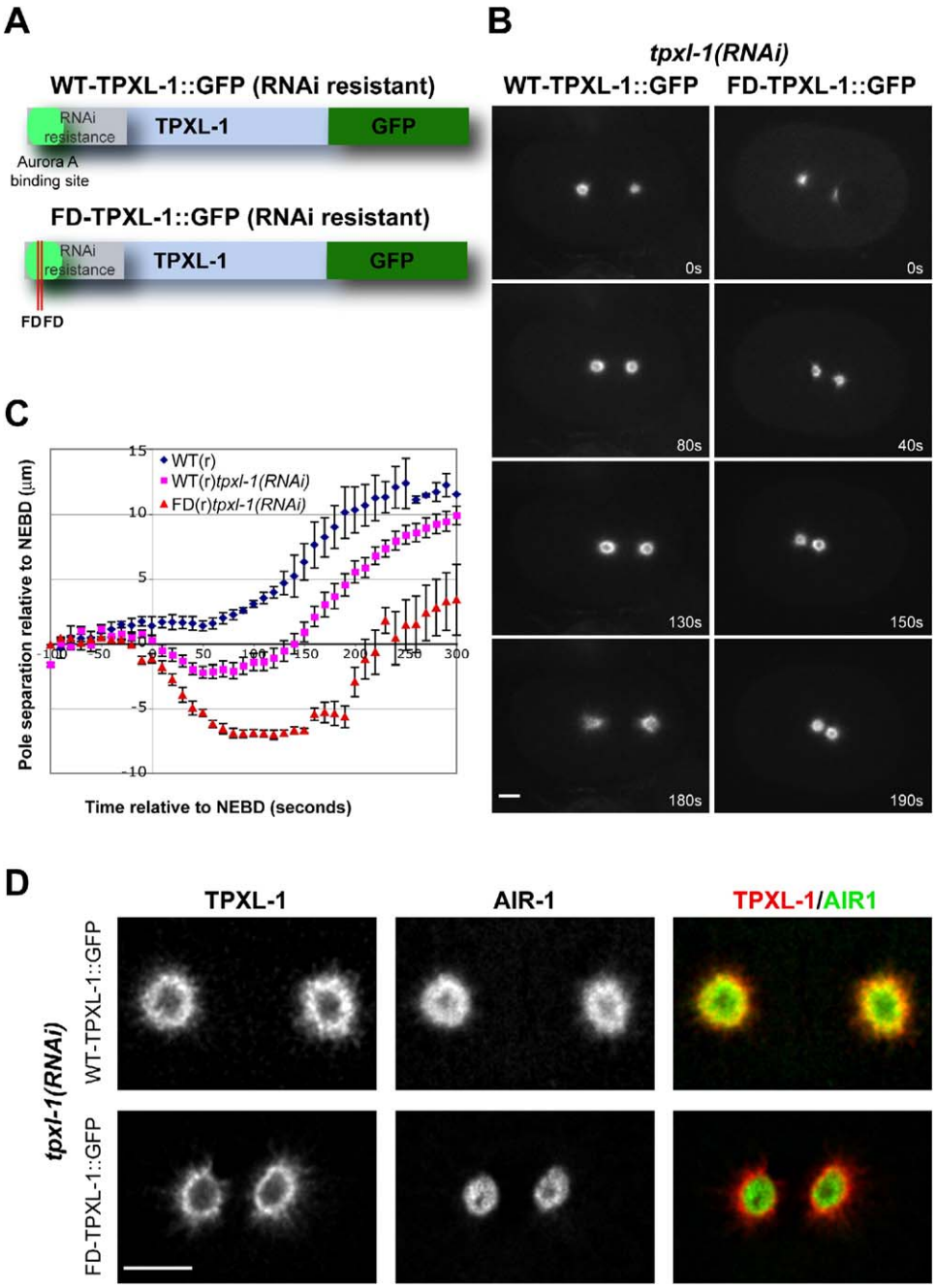

Figure 4. Interaction of TPXL-1 with AIR-1 Is Required for Its Activity In Vivo

(A) Schematic of transgenes: RNAi-resistant wild-type TPXL-1 (blue box) was fused to GFP (dark green box) (top). The Aurora A binding site is indicated in the light green box. The RNAi-resistance tag was created by insertion of silent mutations into the N terminus (gray box). To specifically deplete the endogenous TPXL-1, dsRNA was raised against this region. The RNAi-resistant mutant TPXL-1::GFP transgene (bottom) is as described in the wild-type transgene. F15D and F18D mutations are indicated by red lines in the Aurora A binding site.

(B) Selected panels from time-lapse recordings of wt TPXL-1::GFP(r) and FD TPXL-1::GFP(r)-expressing embryos after *tpxl-1(RNAi)* to remove endogenous TPXL-1. Centrosomal fluorescence intensities are similar in both embryos (Figure S1C). The poles were completely collapsed in the FD TPXL-1::GFP(r)-expressing embryo, but not in the wt TPXL-1::GFP(r)-expressing embryo. Times are in seconds relative to NEBD. See also Movies S6 and S7.

(C) Spindle-pole separation relative to NEBD was tracked for transgenic embryos: wt TPXL-1::GFP(r) (n = 2) and FD TPXL-1::GFP(r) (n = 2) (plotted together; blue diamonds); *tpxl-1(RNAi)* in wt TPXL-1::GFP(r) (n = 7) (pink squares), and *tpxl-1(RNAi)* in FD TPXL-1::GFP(r) (n = 6) (red triangles). Average pole-to-pole distance at NEBD was set to zero. Error bars are standard error of the mean (SEM) with a confidence interval of 0.95.

(D) High-magnification view of centrosomes from a metaphase wt TPXL-1::GFP(r)-expressing embryo after RNAi-mediated depletion of endogenous TPXL-1 (top) and from a FD TPXL-1::GFP(r)-expressing embryo after RNAi-mediated depletion of endogenous TPXL-1 (bottom). Embryos were stained for TPXL-1 (red) and AIR-1 (green). In *tpxl-1(RNAi)* wt TPXL-1::GFP(r), AIR-1 localizes to the peripheral centrosomal region. In the *tpxl-1(RNAi)* FD TPXL-1::GFP(r) embryo, AIR-1 localizes to the inner centrosomal region. All images are single z sections of deconvolved wide-field data sets. Abbreviation: r, RNAi resistant. Bars: B, 5 μm; D, 3 μm.

Table 1. Comparison of AIR-1- and TPXL-1-Depletion Phenotypes (The Cellular Process in the Left Column Is Affected [+] or Not Affected [–] upon Protein Depletion).

	AIR-1	TPXL-1
Cell Polarity	+[a,c]	–
Centrosomal γ-Tubulin Recruitment	+[b]	–
Robust Aster Formation	+[b]	+
Spindle Assembly	+[a,b]	+
Spindle Elongation at Anaphase	+[b]	–

[a] Schumacher et al., 1998
[b] Hannak et al., 2001
[c] C. Cowan and A.A.H., unpublished data.

dent manner (Gruss and Vernos, 2004). By using two different tests, we showed that TPXL-1 is not required for chromatin-dependent microtubule nucleation. First, in *spd-5* mutant embryos, which lack functional centrosomes, microtubules assemble around mitotic chromosomes and are unable to form a spindle-like structure (Figure S3A; Hamill et al., 2002). In *spd-5(RNAi);tpxl-1 (RNAi)* embryos, we still observed these chromatin-associated microtubules (Figure S3A). Subsequent immunofluorescence assays revealed the efficient depletion of both proteins (Figure S4A). Thus, at the level of depletion in *tpxl-1(RNAi*) embryos in which spindles collapse, noncentrosomal microtubules are still present. Second, during *C. elegans* female meiosis, microtubules nucleate around the chromosomes and subsequently organize into bipolar spindles that lack astral microtubules (Albertson and Thomson, 1993). *tpxl-1 (RNAi)* resulted in loss of all meiotic spindle TPXL-1 staining, but meiotic spindle morphology was indistinguishable from wild-type embryos (Figure S3B). Therefore, we conclude that inhibition of chromatin-stimulated microtubule nucleation is unlikely to be the origin of the spindle collapse observed in TPXL-1-depleted embryos. This suggests that the mechanism of spindle stabilization by TPXL-1 is different from that of TPX2 in *Xenopus* extracts.

TPXL-1 Is Not Required for Generation of Astral Forces

Because TPXL-1 is not required for microtubule assembly around chromatin, we searched for an alternate explanation for the observed spindle-collapse phenotype. During spindle assembly, a balance of outward and inward forces exerted on spindle poles controls spindle length. One possibility is that TPXL-1 contributes to cortical pulling forces, transmitted by astral microtubules. In this idea, kinetochore-mediated pulling forces would dominate over weakened astral pulling forces, resulting in spindle collapse. To test if the astral pulling forces are active in *tpxl-1(RNAi)* embryos, we performed spindle-severing experiments with a UV laser (Grill et al., 2001). In wild-type embryos, astral forces pull spindle poles apart after laser-mediated spindle severing (Figures 5A–5C). In TPXL-1-depleted embryos, the spindle poles separated from each other with peak velocities comparable to wild-type (Figure 5C) and the final positions of the centrosomes postablation were similar to wild-type (Figures 5A and 5B). From these results, we conclude that astral forces are not affected by the depletion of TPXL-1.

Kinetochore Microtubules Form after RNAi of TPXL-1

The results so far suggest an intrinsic problem in spindle stability in the absence of TPXL-1. Kinetochore function is required for the formation of a stable spindle by providing a mechanical connection between replicated chromosomes and both spindle poles (Oegema et al., 2001). To resolve the morphology of the collapsed spindles, we performed electron tomography on *tpxl-1(RNAi)* embryos after spindle collapse (Figure 6A). EM-tomography revealed that a spindle is formed and centrosomes are connected to kinetochore microtubules but that these kinetochore microtubules are extremely short.

Spindle Collapse in *tpxl-1(RNAi)* Embryos Depends on Intact Kinetochores, but Not Antiparallel Microtubules

Could kinetochore microtubule instability be causing the spindle collapse? In CeCENP-A-depleted embryos, kinetochore assembly fails and poles separate prematurely before forming a metaphase spindle (Oegema et al., 2001; Figure 6B, compare wild-type and CeCENP-A-depleted 160 s; Figure 6C). In double RNAi, TPXL-1- and CeCENP-A- (Figure 6B) or TPXL-1- and CeCENP-C- (data not shown) depleted embryos, pole separation occurs as in CeCENP-A-depleted embryos, with spindle poles prematurely elongating (Figure 6B, 90 s and 160 s; Figure 6C). Subsequent immunofluorescence assays confirmed that in double RNAi embryos, TPXL-1 was depleted as efficiently as in single *tpxl-1(RNAi)* embryos (Figure S4B). Thus, the spindle collapse in *tpxl-1(RNAi)* embryos is mediated by kinetochores pulling the poles toward the chromosomes.

To check that the spindle collapse in TPXL-1-depleted embryos occurs by destabilization of kinetochore-attached microtubules and not by overlapping antiparallel microtubules emanating from opposite spindle poles, we analyzed spindle formation in *tpxl-1(RNAi)* monopolar spindles. To generate monopolar spindles, we used a *zyg-1(b1)* mutant in which centrosome duplication fails (O'Connell et al., 2001). These mutants make half spindles and therefore have no overlapping antiparallel microtubules. However, spindles still collapse in *tpxl-1(RNAi);zyg-1* double mutants (Figure 6D).

Abnormal Microtubule Behavior at Spindle Poles in *tpxl-1(RNAi)* Embryos

Why are kinetochore microtubules unstable in *tpxl-1(RNAi)*? Aurora A is localized at spindle poles, suggesting that defects in spindle-pole organization could contribute to a lack of kinetochore microtubule stability. To investigate microtubule behavior at spindle poles, we utilized EBP-2::GFP (an EB1 homolog that specifically decorates growing microtubule ends; Srayko et al., 2005). We first examined microtubule nucleation rates. Surprisingly, we found that the microtubule nucleation rate in *tpxl-1(RNAi)* embryos was not significantly different from wild-type embryos (90 ± 12% of wild-type metaphase nucleation rates; $p = 0.25$; Figure 7A) despite a reduced microtubule intensity at spindle poles (Figure S2C). This suggested that the decrease in microtubule levels at centrosomes in *tpxl-1(RNAi)* results from a lack of persistence and/or stability of nu-

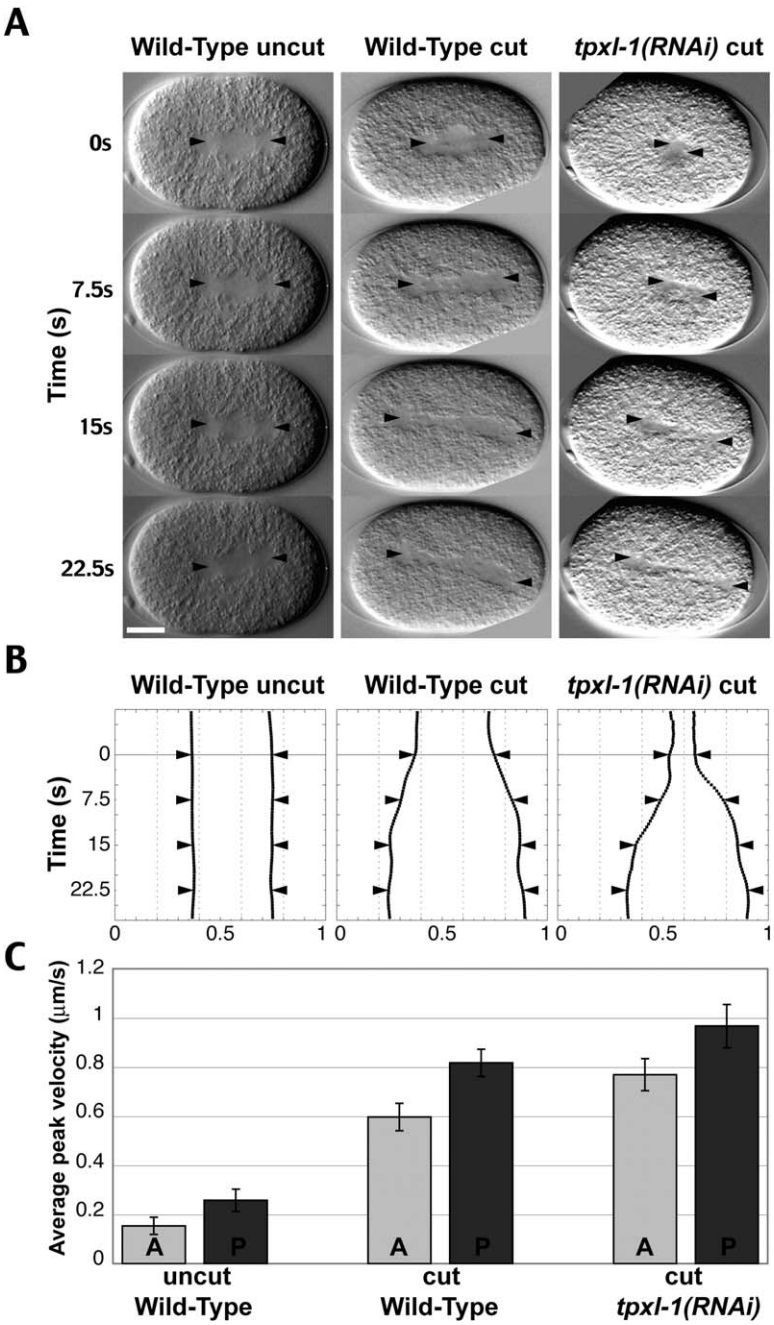

Figure 5. TPXL-1 Is Not Required for Generation of Astral Forces

(A) Laser cutting of spindles to monitor astral pulling forces. Summarization of differential interference contrast (DIC) time-lapse movies of uncut wild-type (left column), laser-cut wild-type (middle column), and laser-cut *tpxl-1(RNAi)* (right column) embryos. The laser-cut was performed at 0 s at the midline between the spindle poles. See also Movies S12 and S13.

(B) Spindle-pole tracking of embryos shown in (A). Position is relative to the embryo length: 0 represents anterior cortex, 1 represents posterior cortex.

(C) Average peak velocities of anterior and posterior spindle poles. Error bars are SEM with a confidence interval of 0.95. Average peak velocities were measured for eight wild-type uncut, 15 wild-type cut, and 23 *tpxl-1(RNAi)* cut. Bar: 10 μm.

cleated microtubules rather than a defect in microtubule nucleation.

We also noticed an increase in the frequency of EBP-2::GFP dots exhibiting a switch from anterograde movement (growth away from centrosomes) to retrograde movement (movement toward centrosomes) (see Movie S20). The switch occurs at low frequency in wild-type (see Movie S19). Because EBP-2::GFP only associates with growing microtubule plus ends, retrograde movements are thought to be a consequence of detached microtubule minus ends (Srayko et al., 2005). In *tpxl-1(RNAi)* embryos, we observed a 6-fold increase in retrograde movements in astral microtubules compared to wild-type (Figure 7B). We also observed retrograde EBP-2::GFP movements in bipolar spindles (Figure 7C, yellow dot) and monopolar spindles (see Movie S21) of *tpxl-1(RNAi)* embryos, although it was not feasible to quantify the number due to a high density of EBP-2 dots in the spindle. The increased frequency of these movements in *tpxl-1(RNAi)* embryos suggests that the spindle-collapse phenotype observed may arise from a loss of microtubule minus-end stability near the centrosomes.

Discussion

The data presented here provide two key pieces of evidence that identify the first ortholog of TPX2 in inverte-

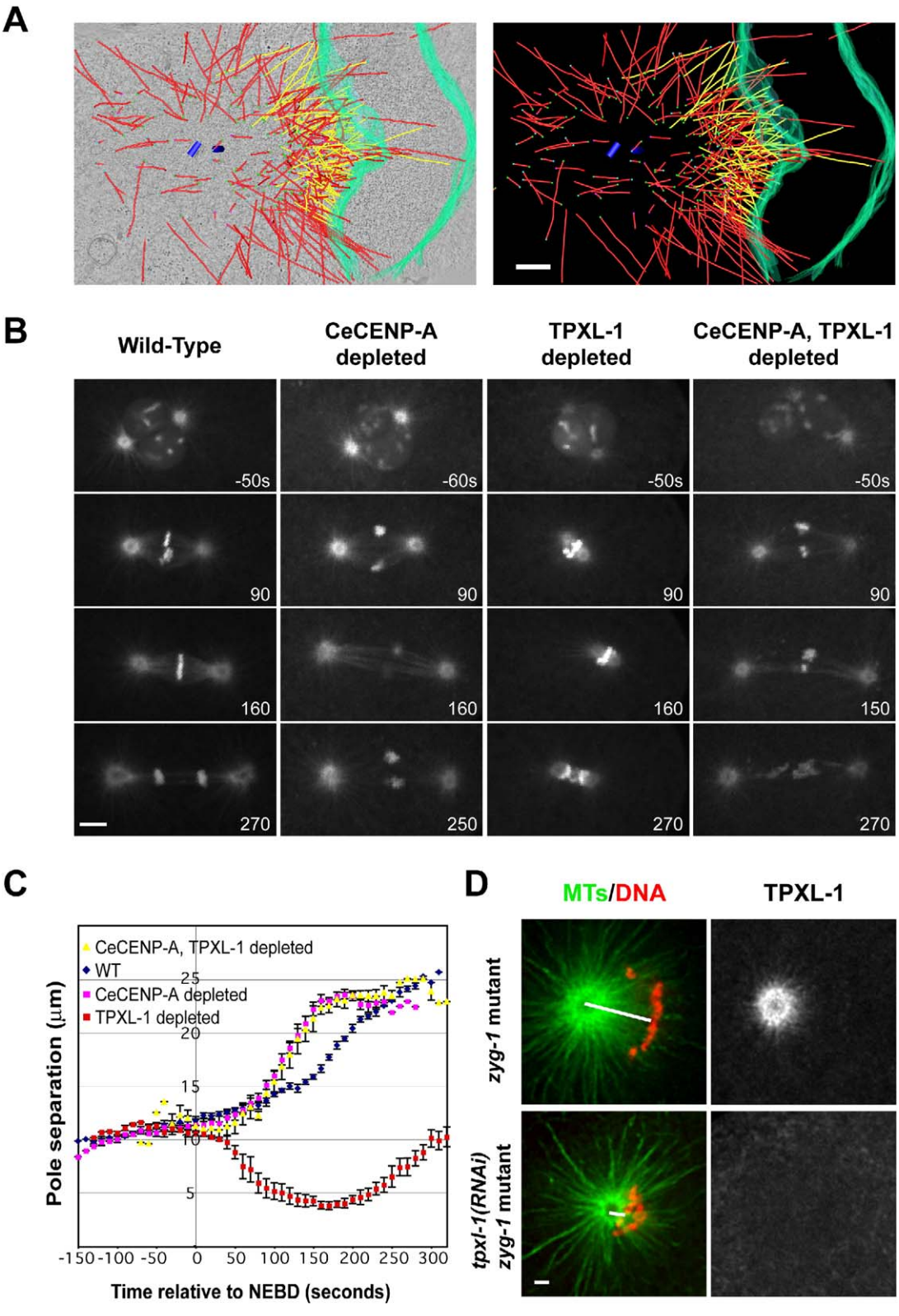

Figure 6. Spindle Collapse in *tpxl-1(RNAi)* Embryos Depends on Intact Kinetochores, but Not Antiparallel Microtubules

(A) Kinetochore microtubules still form in the absence of TPXL-1. Electron tomography of a collapsed *tpxl-1(RNAi)* spindle. The 3D model superimposed on a selected tomographic slice is shown in the left panel. The partial reconstruction was computed from a 2 × 1 montage. The 3D model (right) shows the boundaries of a chromosome (green) and the position of spindle microtubules (red, yellow lines). Microtubules that ended on the chromosome were defined as kinetochore microtubules (yellow).

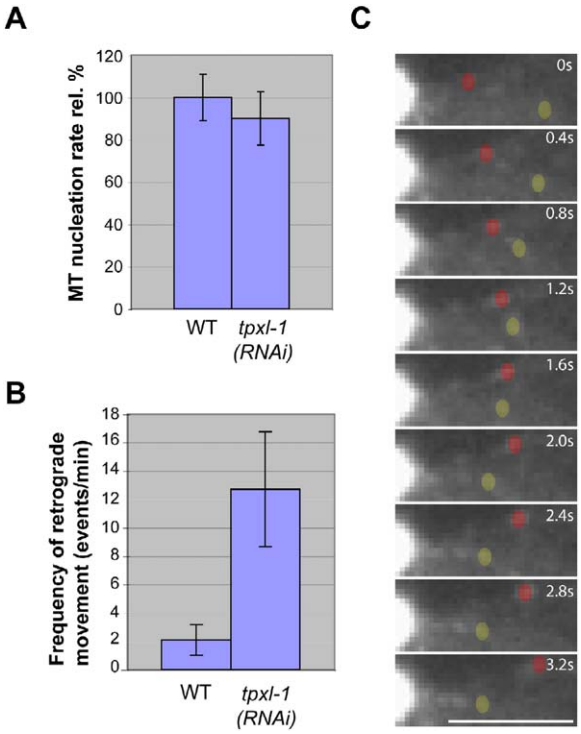

Figure 7. Abnormal Microtubule Behavior at Spindle Poles in *tpxl-1(RNAi)* Embryos

(A) Quantification of astral microtubule nucleation rates in wild-type and *tpxl-1(RNAi)* embryos expressing EBP-2::GFP (an EB1 homolog that specifically decorates growing MT ends). Kymographs from 1 min stream-acquisition movies were used to quantify the number of EBP-2::GFP dots emanating from metaphase centrosomes (Srayko et al., 2005). Nucleation rates are relative to wild-type metaphase (% wt MTs/min). Standard error at 95% confidence is shown; wild-type, n = 16; *tpxl-1(RNAi)*, n = 10.

(B) Frequency of retrograde movements (events/min) of EBP-2::GFP dots in wild-type and *tpxl-1(RNAi)* embryos is shown. Standard error at 0.95 confidence is shown; wild-type, n = 16; *tpxl-1(RNAi)*, n = 12.

(C) A series of images from a stream-acquisition movie of a EBP-2::GFP dot exhibiting retrograde movement (colored yellow) and a separate dot exhibiting normal anterograde growth movement (colored red) within the mitotic spindle of a *tpxl-1(RNAi)* embryo is shown. Centrosome is on the left (white circle). See also Movie S20, for astral retrograde movements and Movie S21, for retrograde movements in a monopolar spindle. Bar: 5 μm.

brates. First, both proteins interact with Aurora A and stimulate its kinase activity in vitro (Bayliss et al., 2004; Eyers et al., 2003; Tsai et al., 2003). Second, both proteins are required for the localization of Aurora A to spindle microtubules, but not for the localization of Aurora A to the spindle pole (Kufer et al., 2002). However, we have not been able to find any evidence that TPXL-1 is regulated through the Ran pathway, as is the case for TPX2. Although TPXL-1 contains a putative nuclear localization sequence, we do not see prominent nuclear localization. The phenotype of Ran depletion is the failure to form a mitotic spindle, reminiscent of the loss of kinetochore function and unlike the phenotype of TPXL-1 depletion (Askjaer et al., 2002; Bamba et al., 2002). More work is required to characterize the contribution of this pathway to spindle assembly in *C. elegans*.

The identification of a TPX2 ortholog has allowed us to resolve an important question: is a TPX2-Aurora A interaction required for TPX2 function during spindle assembly? In *Xenopus* extracts, the C terminus of TPX2 lacking the Aurora A binding site can complement TPX2 function (Brunet et al., 2004). In human cells, the mitotic arrest induced by Aurora A RNAi has made it difficult to compare the phenotype of Aurora A RNAi and TPX2 RNAi. Our results show that mutated TPXL-1, which cannot bind to Aurora A, does not rescue the spindle-collapse defect. Therefore, in *C. elegans* mitosis, an essential function of the TPX2 ortholog is to target Aurora A to spindles.

Why do spindles collapse in the absence of TPXL-1? In *Xenopus* egg extract, TPX2 is required for chromatin-dependent microtubule nucleation. However, in *C. elegans*, under RNAi conditions in which spindles collapse, microtubule nucleation around chromosomes is unaffected. Thus, TPX2 appears to function differently in *Xenopus* and *C. elegans*. We do not know the reason for this difference. Perhaps TPX2 can activate different kinases in different systems. Alternatively, the C terminus of TPX2 may have functions unrelated to Aurora A activity, and these functions may be more essential in *Xenopus* extracts.

Our data suggest that the most likely reason that spindles collapse in the absence of TPXL-1 is destabilization of kinetochore microtubules. One possibility is that the kinetochore-attached plus ends are unstable in the absence of TPXL-1. Unfortunately, the high-turnover rate of microtubules in *C. elegans* prophase precludes testing this model by FRAP (A.D., unpublished observations; Srayko et al., 2005). The fact that TPXL-1 operates together with Aurora A and Aurora A is localized to spindle poles suggests that the primary defect of *tpxl-1(RNAi)* could be in organization of the spindle pole. Supporting evidence for this is that the number of microtubules at centrosomes is quite reduced, whereas the nucleation rate seems to be the same as wild-type, and that a substantial number of polymerizing microtubules exhibit freedom of movement (visible as retrograde plus-end movement) inconsistent with a stable

(B) Summarization of time-lapse sequences of wild-type (first column), CeCENP-A-depleted (second column), TPXL-1-depleted (third column), and CeCENP-A- and TPXL-1-depleted (fourth column) embryos expressing GFP::β-tubulin and GFP::histone. Times are in seconds relative to NEBD (left). See also Movies S15–S18.

(C) Spindle pole separation relative to NEBD. The graph shows the average pole-to pole-distance of wild-type (blue), CeCENP-A-depleted (pink), TPXL-1-depleted (red), and CeCENP-A- and TPXL-1-depleted (yellow) embryos. Error bars are SEM with a confidence interval of 0.95 (n = 4).

(D) Chromosomes in monopolar spindles collapse into the centrosomes after TPXL-1 depletion. Half spindles from a *zyg-1* mutant (top) and a *tpxl-1(RNAi);zyg-1* mutant embryo (bottom) stained for microtubules and DNA (left) and TPXL-1 (right) are shown. The white line indicates chromosome-pole distance. Images are single z sections of deconvolved, wide-field data sets. Bars: A, 500 nm; B, 5 μm; D, 1 μm.

attachment to centrosomes. Perhaps the minus ends of microtubules are unstable, and this allows the centrosomes to be pulled toward the chromosomes.

Therefore, we propose that in C. *elegans* mitosis, the homolog of TPX2— TPXL-1— targets Aurora A to the spindle, where it phosphorylates downstream targets required for kinetochore microtubule stabilization. These could be centrosome, spindle, or kinetochore components. One possible candidate is TAC-1, a protein implicated in microtubule stability (Bellanger and Gonczy, 2003; Le Bot et al., 2003; Lee et al., 2001; Srayko et al., 2003) whose homologs are known to be an Aurora A substrate (Giet et al., 2002). TPX2 itself is a microtubule binding protein (Wittmann et al., 2000), so it is possible that phosphorylation of TPXL-1 by Aurora A may also contribute to the stabilization activity. The other known substrate of Aurora A, the motor protein Eg5 (Giet et al., 1999), is not required for *C. elegans* spindle assembly (Bishop et al., 2005). Identification of other Aurora A substrates would provide important insights into the mechanisms of spindle assembly.

C. elegans Aurora A has a number of different roles in the first embryonic cell division: (1) cell polarity, (2) centrosome maturation, (3) spindle assembly, and (4) spindle elongation at anaphase. In contrast, TPXL-1 is required only for spindle assembly, and the rescue experiments with wild-type or mutant TPXL-1 indicate that all of the functions of TPXL-1 are contained within a subset of Aurora A functions (Table 1). Thus, it seems that a key role for Aurora A in spindle assembly is to stabilize microtubules nucleated from centrosomes that are bound to kinetochores. Because RNAi is a rundown technique, it is possible that the difference between Aurora A phenotypes and TPX2 phenotypes represents a difference in sensitivity of different Aurora A functions to TPX2 levels. However, we think it is more likely that other Aurora A activation and targeting subunits exist that are responsible for the various functions of Aurora A. In this way, the cell can ensure that Aurora A is targeted at the correct time and to the correct place during the cell cycle to perform its various roles.

Experimental Procedures

RNA-Mediated Interference

For production of *tpxl-1* dsRNA, the gene was amplified from either N2 genomic DNA or the cDNA yk1152d5. RNA synthesis and annealing were performed by using standard procedures (Oegema et al., 2001). Primer sequences are listed in Table S1. L4 hermaphrodites were injected with dsRNA and incubated for 45–48 hr at 16°C, 30–36 hr at 20°C, or 24 hr at 24.5°C before being examined.

GFP Strains and RNAi Resistance Transgenes

The following GFP strains used were as previously described: AZ244, GFP::β-tubulin, (Praitis et al., 2001); XA3501, GFP::tubulin; GFP::Histone, (Askjaer et al., 2002); and TH24, GFP::γ-tubulin, (Hannak et al., 2002). TH41 (GFP::AIR-1) was a gift from Carrie Cowan (MPI-CBG, Dresden, Germany). The strain *spd-5(or213ts)* (Hamill et al., 2002) was crossed to the strain AZ244 to obtain *spd-5* mutant embryos expressing GFP::β-tubulin.

The strain TH53 expressing TPXL-1::GFP was constructed by high-pressure particle bombardment (Bio-Rad) of DP38 [*unc-119(ed3)*] worms with a plasmid (a gift from Andrei Pozniakovski, MPI-CBG, Dresden, Germany) containing a C-teminal TPXL-1::GFP fusion gene under the control of the *pie-1* promoter and *unc-119(+)* as a selection marker (Praitis et al., 2001). TH53 likely contains an integrated array of the rescuing plasmid due to 100% rescue of progeny for *unc*-119, and all progeny examined express GFP.

RNAi-resistant wild-type and FD TPXL-1::GFP transgenes were made as follows: The first 500 bp of the *tpxl-1* sequence were synthesized by Geneart GmbH (Regensburg, Germany). This sequence contained silent mutations such that the synthetic gene diverged from the original gene at the DNA level (28% divergent), but not at the protein-coding level. Wherever possible, the codon usage was adapted to the codon bias of *Caenorhabditis elegans* genes. A second *tpxl-1(RNAi)*-resistant gene was synthesized containing F15D, F18D mutations. The first 500 bp of the *tpxl-1* sequence in the TPXL-1::GFP construct were then excised by using a unique restriction site and were replaced with newly synthesized genes. The transgenic worms were generated as explained above. To specifically silence the endogenous gene in these transgenic worms, dsRNA was synthesized against 3–393 bp of *tpxl-1*.

Electron Tomography and 3D modeling

Sample preparation for electron tomography was carried out essentially as published (O'Toole et al., 2003). Briefly, RNAi worms were high-pressure frozen (BAL-TEC HPM 010), freeze substituted (Leica EM AFS), and thin-layer embedded in Epon and Araldite for serial sectioning. Electron tomography was performed on 300 nm plastic sections of *tpxl-1(RNAi)* embryos with a TECNAI F30 intermediate-voltage electron microscope operated at 300 kV. Tomograms were computed and analyzed by using the IMOD software package as published (O'Toole et al., 2003).

Time-Lapse Microscopy and Quantification

TPXL-1::GFP-, GFP::β-tubulin-, and GFP::β-tubulin;GFP::histone-expressing embryos were imaged with a spinning disk confocal microscope controlled by the Metamorph Imaging software. Images were acquired every 8 or 10 s with an ORCA 100 (Hamamatsu) camera and 63×, 1.4 NA PlanApochromat objective with 500–1,000 msec exposure time. GFP::γ-tubulin-expressing embryos were imaged with a wide-field microscope (Zeiss Axioplan II) equipped as described above. Images were acquired every 10 s with 550 msec exposure time and 2× binning. Quantification of centrosomal β-tubulin and γ-tubulin was performed as previously described (Pelletier et al., 2004).

Spindle Severing

Spindle severing was performed as described previously (Grill et al., 2001) with a pulsed, third-harmonic, solid-state UV laser (λ = 354 nm, 4 ns, 12 μJ/Pulse, PowerChip, JDS Uniphase). DIC images were acquired every 0.5 s with an inverted microscope (Axiovert 200M, Zeiss) with a water-immersion lens (C-Apochromat 63×, NA 1.2, Zeiss) (Grill et al., 2003). Spindle pole tracking and analysis were performed as described (Grill et al., 2001).

Protein and Antibody Production

For generating antibodies against TPXL-1, the GST::TPXL-1 (aa 1–210) was affinity purified after expression of the appropriate cDNA fragment cloned into pGEX6P-1 (Amersham). Antibodies to the N-terminal TPXL-1 (aa 1–210), the C-terminal 17 amino acids of TPXL-1, and the C-terminal 12 amino acids of AIR-1 were raised, affinity purified, and directly labeled as described (Oegema et al., 2001).

For GST pull-down assays, GST::TPXL-1 (aa 1–63) was affinity purified after expression of the specified cDNA fragment cloned into pGEX-M8 (a gift from Mike Tipsword; MPI-CBG, Dresden, Germany). F15D, F18D GST::TPXL-1 (aa 1–63), and V23D,Y26D GST::TPXL-1 (aa 1–63) site-directed mutants were generated by using the QuikChange protocol (Stratagene). For double mutants, residues were substituted in two steps, and the resulting constructs were confirmed by DNA sequencing (DNA Sequencing Facility, MPI-CBG, Dresden, Germany). GST fusions were expressed in BL21 or BL21 CodonPlus RP *E. Coli* (Stratagene) and purified under native conditions with glutathione agarose beads (Sigma).

Full-length AIR-1 was amplified from first-strand cDNA. The amplified product was subcloned into pGEM-T (Promega) and cloned into pHAT to generate His-tagged AIR-1. His-tagged AIR-1 was ex-

pressed in BL21 *E. Coli* (Stratagene) and purified by using TALON resin (Clontech).

Western Blotting for RNAi and Fixed Imaging

For Western blotting, 20–35 *tpxl-1(RNAi)*-injected worms and an equal number of control worms were washed three times with M9. To 10 μl of total volume, an equal volume of 2× sodium dodecyl sulfate-polyacrylamide gel electrophoresis (SDS-PAGE) sample buffer was added, and tubes were sonicated for 5 min at 80°C in a waterbath sonicator. The entire volume of lysate was loaded onto an SDS-PAGE gel and analyzed by Western blotting by using 1 μg/ml anti-TPXL-1 and ECL (Amersham) detection of HRP-conjugated anti-rabbit secondary antibody (Bio-Rad Laboratories). For loading control, immunoblots were reprobed with anti-α-tubulin antibody (DM1α, Sigma) and detected with either alkaline-phosphatase-conjugated (Jackson ImmunoResearch Laboratories) or HRP-conjugated anti-mouse secondary antibodies.

Immunofluoresence experiments were performed as described previously (Oegema et al., 2001). Antibodies were used at 1 μg/ml. Images through entire embryos were acquired with a wide-field Delta Vision microscope (Applied Precision), and the images were deconvolved with SoftWorx (Applied Precision).

GST Pulldown Assays

2 μg of wild-type and mutant GST::TPXL-1 proteins were bound to 40 μl of glutathione beads. Worm extract was prepared by sonicating 1 g frozen worm pellets in lysis buffer (1 mM EGTA, 1 mM $MgCl_2$, 50 mM HEPES [pH 7.4], 100 mM KCl, 10% glycerol, 0.05% NP-40, and 1 mM DTT) containing protease inhibitors. Worm extract was incubated with the resin for 1 hr at 4°C, washed four times with lysis buffer, and bound proteins were eluted either by adding reduced glutathione (Sigma) or 40 μl of 2× SDS-PAGE sample buffer. 10 μl from each sample was loaded on an SDS-PAGE gel and analyzed by Western blotting by using 1 μg/ml anti-AIR-1 antibodies, HRP-conjugated anti-rabbit secondary antibody, and ECL detection. For comparison of incubated protein levels, immunoblots were also subsequently probed with anti-GST antibody.

In Vitro Kinase Assays

GST::TPXL-1 (1–63) fusions were incubated with Prescission protease (Amersham) for 10 hr at 4°C. Cleaved 4 μM wt and mutant TPXL-1 (1–63) proteins were incubated with HIS-tagged AIR-1 and 0.2 mg/ml Histone H3 (Roche) in kinase buffer (25 mM Hepes [pH7.4], 100 mM KCl, 5 mM $MgCl_2$, 0.5 mM EGTA, 1 mM DTT, 0.05% Tween-20, and 0.05 mM ATP) including $\gamma[^{32}P]$-ATP for 15 min at 25°C (Bayliss et al., 2003). Samples were analyzed by SDS-PAGE and autoradiography. Quantification of Histone H3 phosphorylation was performed with a Fujifilm BAS-1800II phosphorimager.

Supplemental Data

Supplemental Data including four figures and 21 movies are available online with this article at http://www.developmentalcell.com/cgi/content/full/9/2/237/DC1/.

Acknowledgments

We thank C. Cowan, K. Oegema, L. Pelletier, S. Quintin, A. Schlaitz, J. Stear, and M. Van Breugel for comments on the manuscript. We are very grateful to: E. Conti (European Molecular Biology Laboratory, Heildelberg, Germany) for helpful discussion and Human Aurora A and TPX2 proteins; M. Boxem and M. Vidal (Dana Farber Cancer Institute, Boston, MA) for sharing unpublished data; T. Kapoor (The Rockefeller University, New York, NY) for suggesting the monopolar spindle experiment; S. Grill for help with the laser ablation experiment; Y. Kohara (National Institute of Genetics, Mishima, Japan) for cDNAs used in this study; Neslihan Özlü for help with graphics; C. Cowan, B. Bowerman (University of Oregon, Eugene, OR), and W.M. Saxton (Indiana University, Bloomington, IN) for strains; A. Pozniakovski, M. Tipsword, M. Ruer, and S. Rybina for reagents; and the Hyman lab members for many helpful discussions. This work was supported in part by grant RR00592 from the National Center for Research Resources of the National Institutes of Health to J.R.M.

Received: April 29, 2005
Revised: June 10, 2005
Accepted: July 8, 2005
Published: August 1, 2005

References

Albertson, D.G., and Thomson, J.N. (1993). Segregation of holocentric chromosomes at meiosis in the nematode, Caenorhabditis elegans. Chromosome Res. *1*, 15–26.

Askjaer, P., Galy, V., Hannak, E., and Mattaj, I.W. (2002). Ran GTPase cycle and importins alpha and beta are essential for spindle formation and nuclear envelope assembly in living *Caenorhabditis elegans* embryos. Mol. Biol. Cell *13*, 4355–4370.

Bamba, C., Bobinnec, Y., Fukuda, M., and Nishida, E. (2002). The GTPase Ran regulates chromosome positioning and nuclear envelope assembly in vivo. Curr. Biol. *12*, 503–507.

Bayliss, R., Sardon, T., Vernos, I., and Conti, E. (2003). Structural basis of Aurora-A activation by TPX2 at the mitotic spindle. Mol. Cell *12*, 851–862.

Bayliss, R., Sardon, T., Ebert, J., Lindner, D., Vernos, I., and Conti, E. (2004). Determinants for Aurora-A activation and Aurora-B discrimination by TPX2. Cell Cycle *3*, 404–407.

Bellanger, J.M., and Gonczy, P. (2003). TAC-1 and ZYG-9 form a complex that promotes microtubule assembly in *C. elegans* embryos. Curr. Biol. *13*, 1488–1498.

Bishop, J.D., Han, Z., and Schumacher, J.M. (2005). The *Caenorhabditis elegans* Aurora B kinase AIR-2 phosphorylates and is required for the localization of a BimC kinesin to meiotic and mitotic spindles. Mol. Biol. Cell *16*, 742–756.

Brunet, S., Sardon, T., Zimmerman, T., Wittmann, T., Pepperkok, R., Karsenti, E., and Vernos, I. (2004). Characterization of the TPX2 domains involved in microtubule nucleation and spindle assembly in *Xenopus* egg extracts. Mol. Biol. Cell *15*, 5318–5328.

Cheeseman, I.M., Anderson, S., Jwa, M., Green, E.M., Kang, J., Yates, J.R., 3rd, Chan, C.S., Drubin, D.G., and Barnes, G. (2002). Phospho-regulation of kinetochore-microtubule attachments by the Aurora kinase Ipl1p. Cell *111*, 163–172.

Eyers, P.A., and Maller, J.L. (2004). Regulation of *Xenopus* Aurora A activation by TPX2. J. Biol. Chem. *279*, 9008–9015.

Eyers, P.A., Erikson, E., Chen, L.G., and Maller, J.L. (2003). A novel mechanism for activation of the protein kinase Aurora A. Curr. Biol. *13*, 691–697.

Fraser, A.G., Kamath, R.S., Zipperlen, P., Martinez-Campos, M., Sohrmann, M., and Ahringer, J. (2000). Functional genomic analysis of *C. elegans* chromosome I by systematic RNA interference. Nature *408*, 325–330.

Gadde, S., and Heald, R. (2004). Mechanisms and molecules of the mitotic spindle. Curr. Biol. *14*, R797–R805.

Giet, R., Uzbekov, R., Cubizolles, F., Le Guellec, K., and Prigent, C. (1999). The Xenopus laevis aurora-related protein kinase pEg2 associates with and phosphorylates the kinesin-related protein XlEg5. J. Biol. Chem. *274*, 15005–15013.

Giet, R., McLean, D., Descamps, S., Lee, M.J., Raff, J.W., Prigent, C., and Glover, D.M. (2002). Drosophila Aurora A kinase is required to localize D-TACC to centrosomes and to regulate astral microtubules. J. Cell Biol. *156*, 437–451.

Grill, S.W., Gonczy, P., Stelzer, E.H., and Hyman, A.A. (2001). Polarity controls forces governing asymmetric spindle positioning in the *Caenorhabditis elegans* embryo. Nature *409*, 630–633.

Grill, S.W., Howard, J., Schaffer, E., Stelzer, E.H., and Hyman, A.A. (2003). The distribution of active force generators controls mitotic spindle position. Science *301*, 518–521.

Groen, A.C., Cameron, L.A., Coughlin, M., Miyamoto, D.T., Mitchison, T.J., and Ohi, R. (2004). XRHAMM functions in ran-dependent

microtubule nucleation and pole formation during anastral spindle assembly. Curr. Biol. *14*, 1801–1811.

Gruss, O.J., and Vernos, I. (2004). The mechanism of spindle assembly: functions of Ran and its target TPX2. J. Cell Biol. *166*, 949–955.

Gruss, O.J., Carazo-Salas, R.E., Schatz, C.A., Guarguaglini, G., Kast, J., Wilm, M., Le Bot, N., Vernos, I., Karsenti, E., and Mattaj, I.W. (2001). Ran induces spindle assembly by reversing the inhibitory effect of importin alpha on TPX2 activity. Cell *104*, 83–93.

Hamill, D.R., Severson, A.F., Carter, J.C., and Bowerman, B. (2002). Centrosome maturation and mitotic spindle assembly in *C. elegans* require SPD-5, a protein with multiple coiled-coil domains. Dev. Cell *3*, 673–684.

Hannak, E., Kirkham, M., Hyman, A.A., and Oegema, K. (2001). Aurora-A kinase is required for centrosome maturation in *Caenorhabditis elegans*. J. Cell Biol. *155*, 1109–1116.

Hannak, E., Oegema, K., Kirkham, M., Gonczy, P., Habermann, B., and Hyman, A.A. (2002). The kinetically dominant assembly pathway for centrosomal asters in *Caenorhabditis elegans* is gamma-tubulin dependent. J. Cell Biol. *157*, 591–602.

Hirota, T., Kunitoku, N., Sasayama, T., Marumoto, T., Zhang, D., Nitta, M., Hatakeyama, K., and Saya, H. (2003). Aurora-A and an interacting activator, the LIM protein Ajuba, are required for mitotic commitment in human cells. Cell *114*, 585–598.

Karsenti, E., and Vernos, I. (2001). The mitotic spindle: a self-made machine. Science *294*, 543–547.

Kufer, T.A., Sillje, H.H., Korner, R., Gruss, O.J., Meraldi, P., and Nigg, E.A. (2002). Human TPX2 is required for targeting Aurora-A kinase to the spindle. J. Cell Biol. *158*, 617–623.

Le Bot, N., Tsai, M.C., Andrews, R.K., and Ahringer, J. (2003). TAC-1, a regulator of microtubule length in the *C. elegans* embryo. Curr. Biol. *13*, 1499–1505.

Lee, M.J., Gergely, F., Jeffers, K., Peak-Chew, S.Y., and Raff, J.W. (2001). Msps/XMAP215 interacts with the centrosomal protein D-TACC to regulate microtubule behaviour. Nat. Cell Biol. *3*, 643–649.

Li, S., Armstrong, C.M., Bertin, N., Ge, H., Milstein, S., Boxem, M., Vidalain, P.O., Han, J.D., Chesneau, A., Hao, T., et al. (2004). A map of the interactome network of the metazoan C. elegans. Science *303*, 540–543.

Mitchison, T.J., Maddox, P., Gaetz, J., Groen, A., Shirasu, M., Desai, A., Salmon, E.D., and Kapoor, T.M. (2005). Roles of polymerization dynamics, opposed motors, and a tensile element in governing the length of *Xenopus* extract meiotic spindles. Mol. Biol. Cell *16*, 3064–3076.

O'Connell, K.F., Caron, C., Kopish, K.R., Hurd, D.D., Kemphues, K.J., Li, Y., and White, J.G. (2001). The *C. elegans* zyg-1 gene encodes a regulator of centrosome duplication with distinct maternal and paternal roles in the embryo. Cell *105*, 547–558.

Oegema, K., Desai, A., Rybina, S., Kirkham, M., and Hyman, A.A. (2001). Functional analysis of kinetochore assembly in *Caenorhabditis elegans*. J. Cell Biol. *153*, 1209–1226.

O'Toole, E.T., McDonald, K.L., Mantler, J., McIntosh, J.R., Hyman, A.A., and Muller-Reichert, T. (2003). Morphologically distinct microtubule ends in the mitotic centrosome of *Caenorhabditis elegans*. J. Cell Biol. *163*, 451–456.

Pelletier, L., Ozlu, N., Hannak, E., Cowan, C., Habermann, B., Ruer, M., Muller-Reichert, T., and Hyman, A.A. (2004). The *Caenorhabditis elegans* centrosomal protein SPD-2 is required for both pericentriolar material recruitment and centriole duplication. Curr. Biol. *14*, 863–873.

Praitis, V., Casey, E., Collar, D., and Austin, J. (2001). Creation of low-copy integrated transgenic lines in Caenorhabditis elegans. Genetics *157*, 1217–1226.

Prigent, C., and Giet, R. (2003). Aurora A and mitotic commitment. Cell *114*, 531–532.

Schatz, C.A., Santarella, R., Hoenger, A., Karsenti, E., Mattaj, I.W., Gruss, O.J., and Carazo-Salas, R.E. (2003). Importin alpha-regulated nucleation of microtubules by TPX2. EMBO J. *22*, 2060–2070.

Scholey, J.M., Brust-Mascher, I., and Mogilner, A. (2003). Cell division. Nature *422*, 746–752.

Schumacher, J.M., Ashcroft, N., Donovan, P.J., and Golden, A. (1998). A highly conserved centrosomal kinase, AIR-1, is required for accurate cell cycle progression and segregation of developmental factors in *Caenorhabditis elegans* embryos. Development *125*, 4391–4402.

Sharp, D.J., Rogers, G.C., and Scholey, J.M. (2000). Microtubule motors in mitosis. Nature *407*, 41–47.

Srayko, M., Quintin, S., Schwager, A., and Hyman, A.A. (2003). *Caenorhabditis elegans* TAC-1 and ZYG-9 form a complex that is essential for long astral and spindle microtubules. Curr. Biol. *13*, 1506–1511.

Srayko, M., Kaya, A., Stamford, J., and Hyman, A.A. (2005). Identification and characterization of factors required for microtubule growth and nucleation in the early *C. elegans* embryo. Dev. Cell *9*, this issue, 223–236.

Tournebize, R., Popov, A., Kinoshita, K., Ashford, A.J., Rybina, S., Pozniakovsky, A., Mayer, T.U., Walczak, C.E., Karsenti, E., and Hyman, A.A. (2000). Control of microtubule dynamics by the antagonistic activities of XMAP215 and XKCM1 in *Xenopus* egg extracts. Nat. Cell Biol. *2*, 13–19.

Trieselmann, N., Armstrong, S., Rauw, J., and Wilde, A. (2003). Ran modulates spindle assembly by regulating a subset of TPX2 and Kid activities including Aurora A activation. J. Cell Sci. *116*, 4791–4798.

Tsai, M.Y., Wiese, C., Cao, K., Martin, O., Donovan, P., Ruderman, J., Prigent, C., and Zheng, Y. (2003). A Ran signalling pathway mediated by the mitotic kinase Aurora A in spindle assembly. Nat. Cell Biol. *5*, 242–248.

Wittmann, T., Wilm, M., Karsenti, E., and Vernos, I. (2000). TPX2, A novel *Xenopus* MAP involved in spindle pole organization. J. Cell Biol. *149*, 1405–1418.

Wittmann, T., Hyman, A., and Desai, A. (2001). The spindle: a dynamic assembly of microtubules and motors. Nat. Cell Biol. *3*, E28–E34.